

Electronic Supplementary Information

Lanthanide-Based Porous Coordination Polymers: Syntheses, Slow Relaxation of Magnetization, and Magnetocaloric Effect

Chinmoy Das,[†] Apoorva Upadhyay,^{†,‡} Kamal Uddin Ansari,[†] Naoki Ogiwara,[‡] Takashi Kitao,[‡] Satoshi Horike,^{,‡,§,||} and Maheswaran Shanmugam^{*†}*

[†]Department of Chemistry, Indian Institute of Technology Bombay, Powai, Mumbai 400076, Maharashtra, India

[‡]Department of Chemistry, Texas A&M University, College Station, Texas 77843, USA

[‡] Department of Synthetic Chemistry and Biological Chemistry, Graduate School of Engineering, Kyoto University, Katsura, Nishikyo-ku, Kyoto 615-8510, Japan

[§] Institute for Integrated Cell-Material Sciences (WPI-iCeMS), Institute for Advanced Study, Kyoto University, Yoshida, Sakyo-ku, Kyoto 606-8501, Japan

^{||}AIST-Kyoto University Chemical Energy Materials Open Innovation Laboratory (ChEM-OIL), Kyoto University, Yoshida, Sakyo-ku, Kyoto 606-8501, Japan.

Email: eswar@chem.iitb.ac.in

Table S1. X-ray crystallographic parameters of **1**

1	
Formula	Dy ₂ C ₁₀ H ₂₀ O ₂₀
Size	0.17 × 0.21 × 0.24
System	Orthorhombic
Space group	<i>F ddd</i>
<i>a</i> [Å]	9.6660(19)
<i>b</i> [Å]	15.364(3)
<i>c</i> [Å]	26.987(5)
α [°]	90
β [°]	90
γ [°]	90
<i>V</i> [Å ³]	4007.8(14)
<i>Z</i>	8
ρ_{calcd} [g/cm ⁻³]	2.603
$2\theta_{\text{max}}$	54.9168
Radiation	MoK α
λ [Å]	0.71075
<i>T</i> [K]	133.15(2)
Reflns	3462
Ind. Reflns	1141
reflns with >2 σ (I)	1105
R1	0.0274
wR2	0.0683

Table S2. Continuous Shape measurement (CShM) for complexes **1** and **2**

Complex	Square antiprism	Bicapped trigonal prism
1	1.21570	1.80981
2	1.25421	1.79989

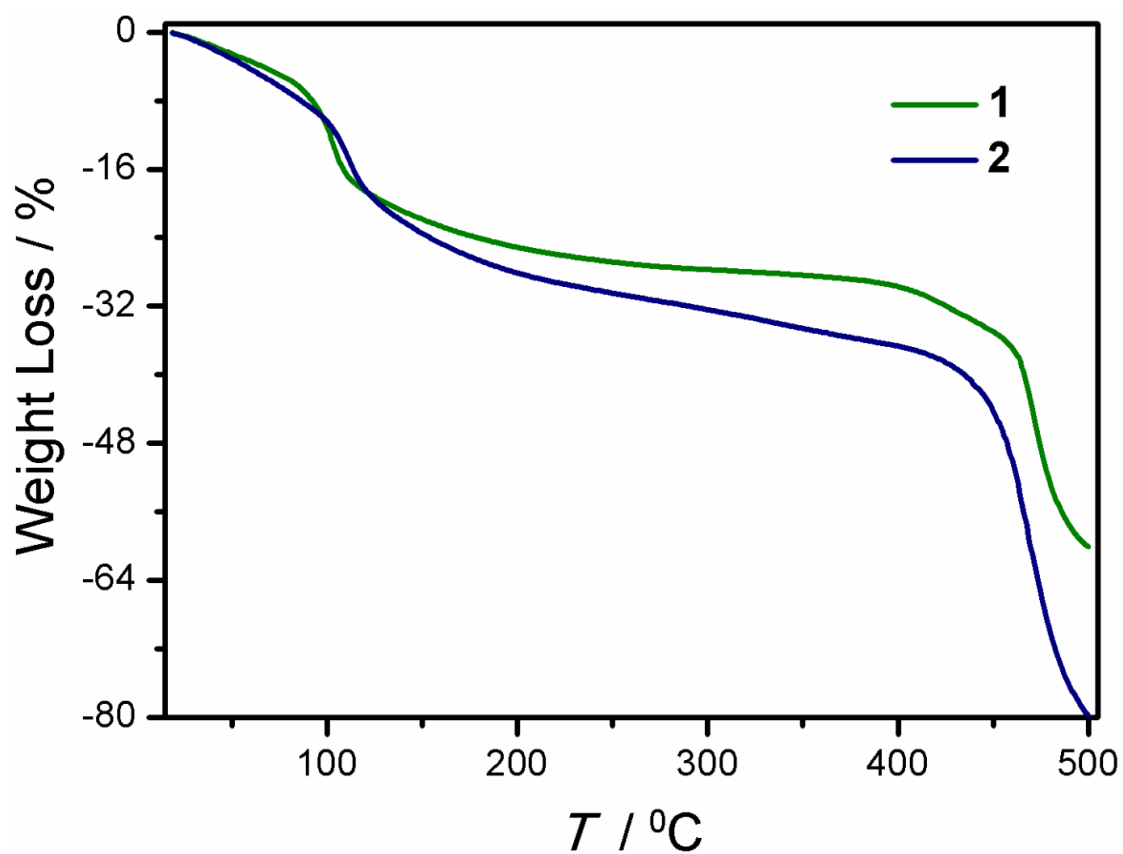


Figure S1. Thermogravimetric analysis (TGA) for the complexes **1** and **2**.

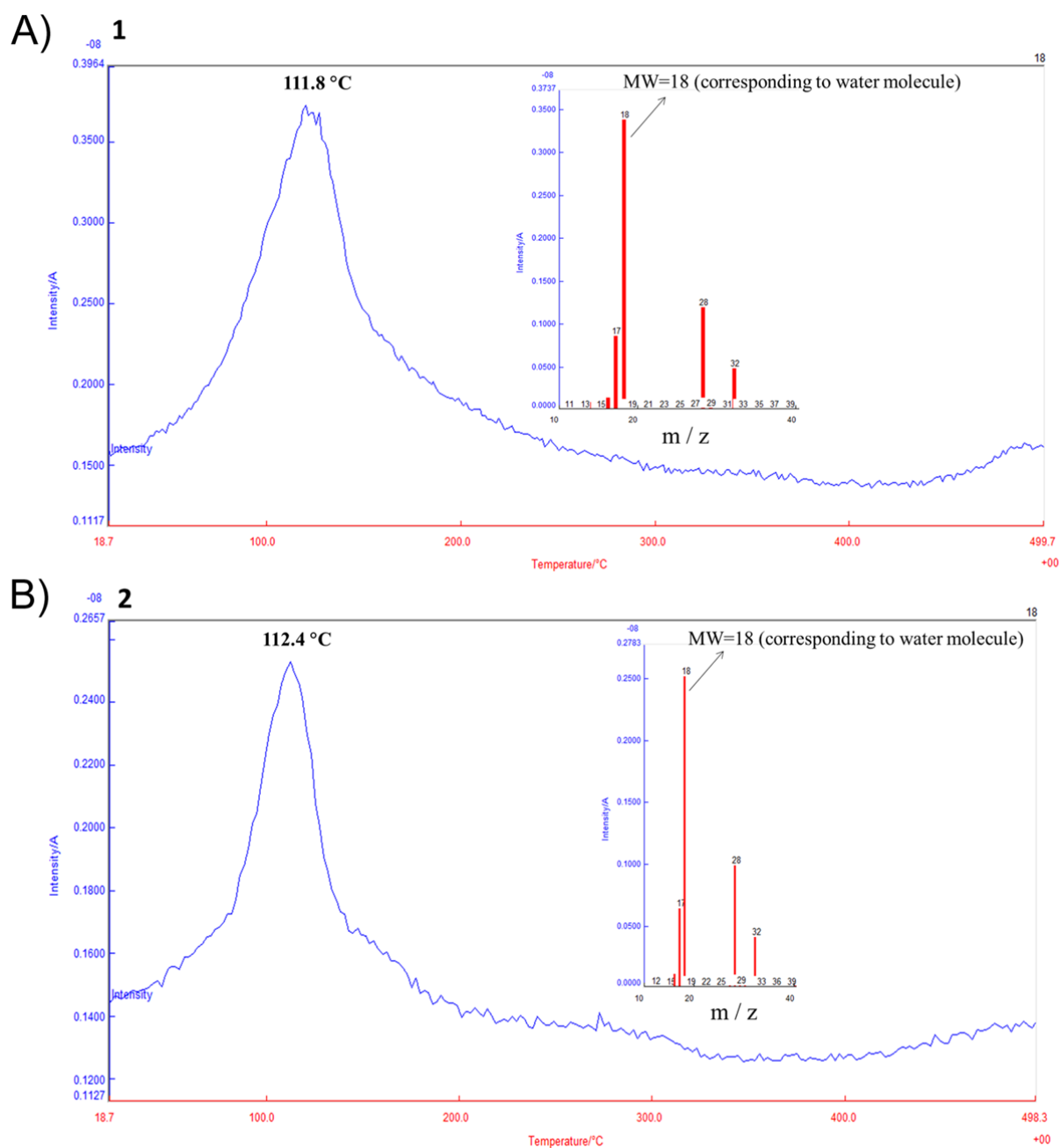


Figure S2. TG-MS analysis for the complexes **1** (panel A) and **2** (panel B). The removal of water molecules evidenced from the ESI-MS analysis shown in the inset.

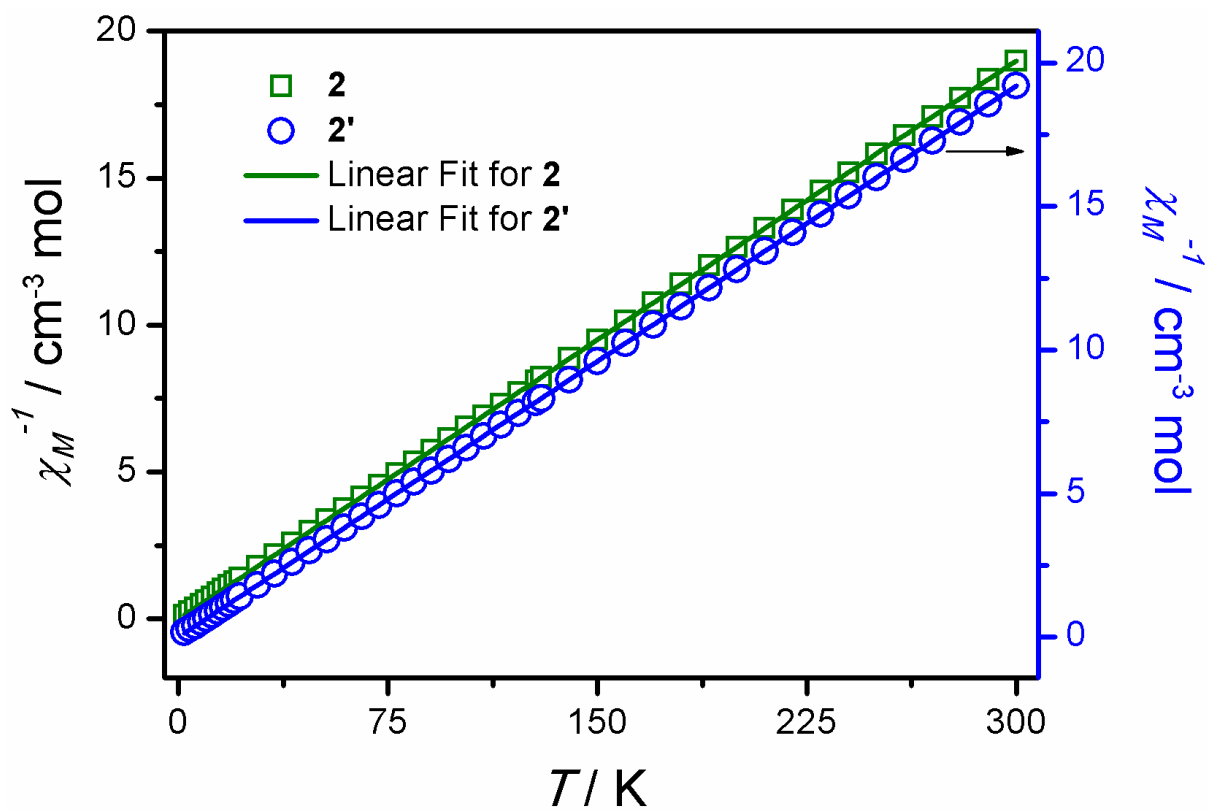


Figure S3. Temperature dependent inverse molar susceptibility (χ_M^{-1}) plot for complex **2** and **2'**. Solid lines represent the linear fit of the magnetic data from 300-2 K.

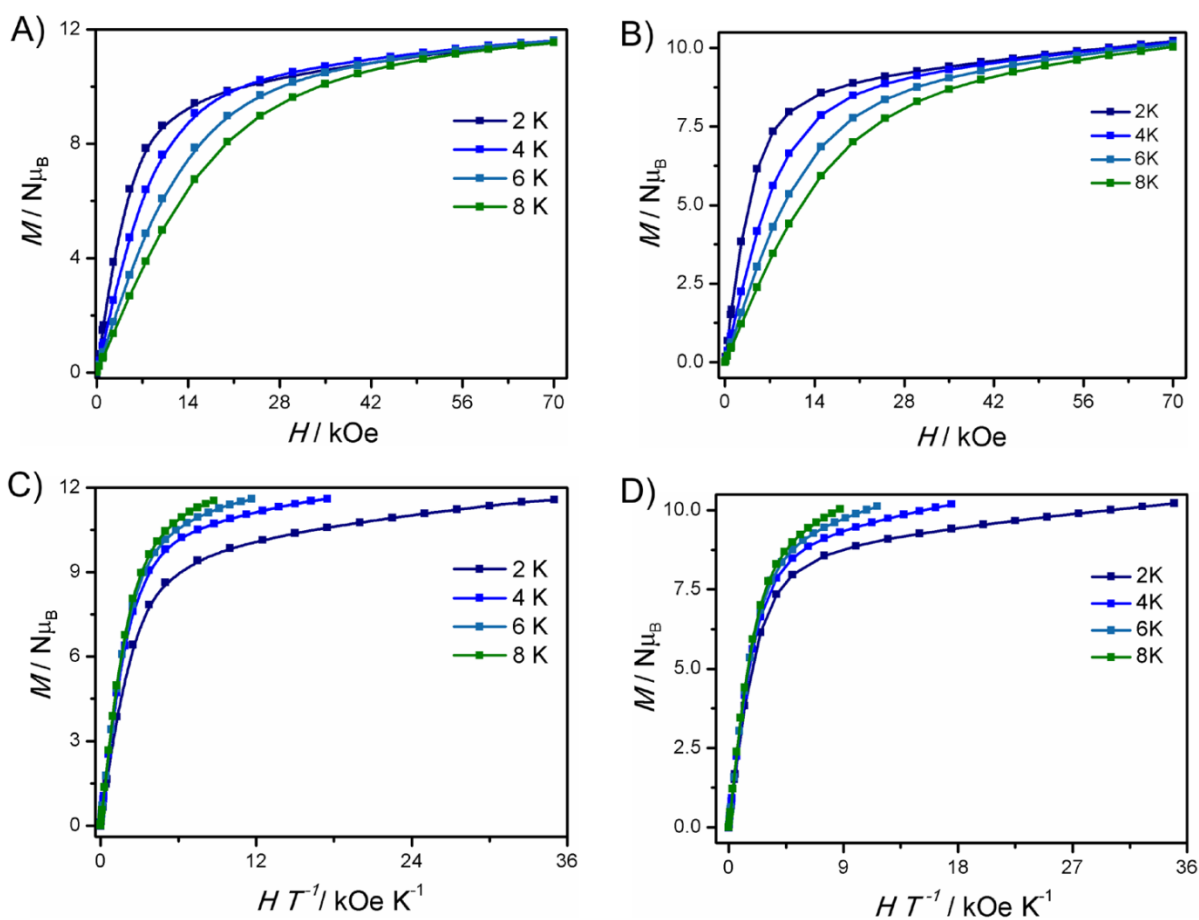


Figure S4. Isothermal field dependant magnetization measurements and reduced magnetization measurements performed on polycrystalline samples of **1** (Panel A and C) and **1'** (Panel B and D) measured from 0-70 *kOe* at the indicated temperature. The solid lines are for eye guides.

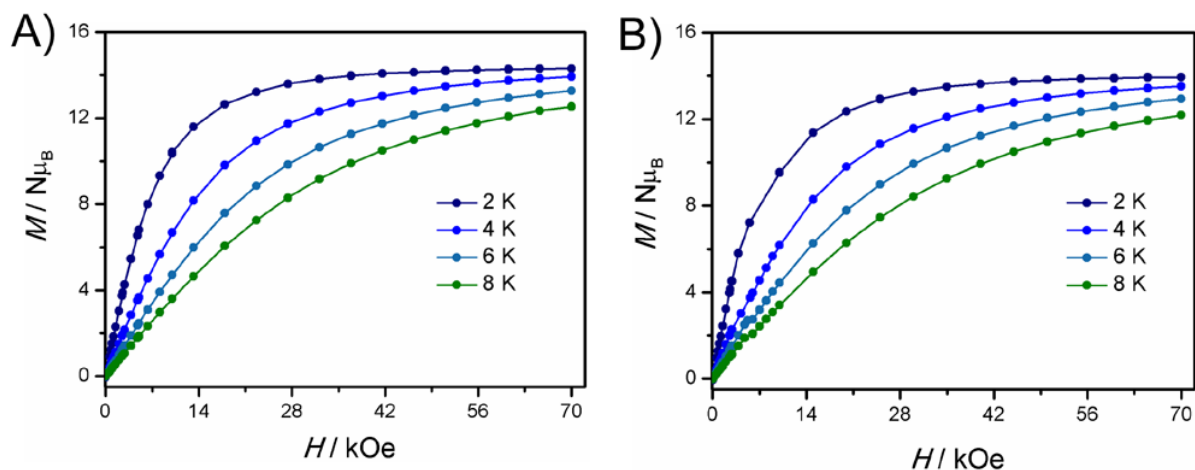


Figure S5. Isothermal field dependant magnetization measurements performed on polycrystalline samples of **2** (Panel A) and **2'** (Panel B) measured from 0-70 kOe at the indicated temperature. The solid lines are for eye guides.

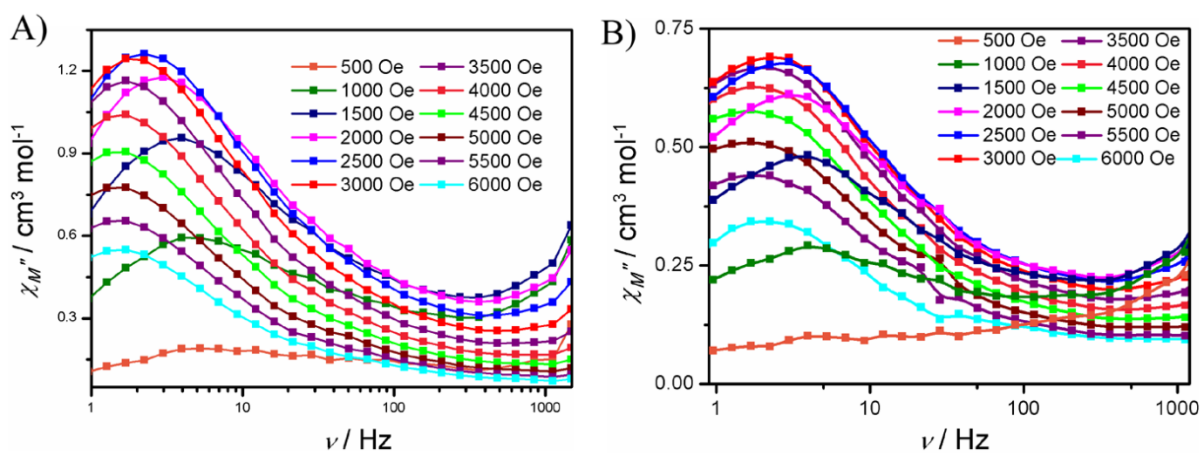


Figure S6. Field dependent out-of-phase ac susceptibility measurement has been performed on powdered sample of complex **1** and **1'**.

Table S3: Fitting parameters for Cole-Cole plot for complex **1** (5.5 kOe bias magnetic field)

S. No.	T (K)	$\chi_{S,tot}$	$\Delta\chi_1$	τ_1	α_1	$\Delta\chi_2$	τ_2	α_2	Residual
1	2.0	0.730944E+00	0.100398E+01	0.192691E-01	0.716252E+00	0.115605E+01	0.11372E+00	0.229971E+00	0.736342E-02
2	2.2	0.109420E-01	0.157115E+01	0.150813E-01	0.760408E+00	0.142661E+01	0.10648E+00	0.296676E+00	0.380790E-02
3	2.4	0.838694E+00	0.559282E+00	0.125135E-01	0.510985E+00	0.167803E+01	0.10047E+00	0.381804E+00	0.106631E-01
4	2.6	0.949435E+00	0.415783E+00	0.746137E-02	0.438115E+00	0.176121E+01	0.918313E-01	0.403042E+00	0.975462E-02
5	2.8	0.950331E+00	0.424506E+00	0.679139E-02	0.451295E+00	0.175207E+01	0.835579E-01	0.400459E+00	0.100564E-01
6	3.0	0.884161E+00	0.518109E+00	0.459761E-02	0.528570E+00	0.171098E+01	0.725915E-01	0.400803E+00	0.100134E-01
7	4.0	0.916780E+00	0.157342E+01	0.228863E-02	0.778695E+00	0.137201E+01	0.421723E-01	0.415426E+00	0.450084E-02
8	5.0	0.772365E-01	0.302822E+01	0.159235E-02	0.895670E+00	0.432938E+00	0.248924E-01	0.319042E+00	0.226003E-02
9	6.0	0.108009E+01	0.377726E+00	0.979087E-03	0.273872E+00	0.904964E+00	0.157913E-01	0.550875E+00	0.145464E-02
10	7.0	0.413518E+00	0.130496E+01	0.825526E-03	0.656650E+00	0.382859E+00	0.124213E-01	0.454363E+00	0.521322E-03
11	8.0	0.126301E+01	0.233671E+00	0.659235E-03	0.182498E+00	0.411182E+00	0.907981E-02	0.542032E+00	0.132772E-02

Table S4: Fitting parameters for Cole-Cole plot for complex **1'** (4.5 kOe bias magnetic field)

S. No.	T (K)	$\chi_{S,tot}$	$\Delta\chi_1$	τ_1	α_1	$\Delta\chi_2$	τ_2	α_2	Residual
1	2.0	0.112118E+01	0.815021E+00	0.222324E-01	0.537109E+00	0.966444E+00	0.14982E+00	0.308507E-02	0.174044E+00
2	2.2	0.114017E+01	0.130003E+01	0.124224E-01	0.613202E+00	0.991915E+00	0.14316E+00	0.116605E+00	0.713041E-02
3	2.4	0.103847E+01	0.110695E+01	0.809273E-02	0.650100E+00	0.112315E+01	0.13568E+00	0.113759E+00	0.128047E-01
4	2.6	0.108196E+01	0.111260E+01	0.648722E-02	0.622655E+00	0.112579E+01	0.12758E+00	0.121939E+00	0.925449E-02
5	2.8	0.106536E+01	0.845617E+00	0.477193E-02	0.595232E+00	0.143935E+01	0.12179E+00	0.211336E+00	0.146813E-01
6	3.0	0.113703E+01	0.108527E+01	0.425223E-02	0.596212E+00	0.116638E+01	0.11487E+00	0.158426E+00	0.779375E-02
7	3.2	0.115618E+01	0.146364E+01	0.349828E-02	0.618005E+00	0.861037E+00	0.10935E+00	0.107585E+00	0.662188E-02
8	3.4	0.119004E+01	0.149488E+01	0.293450E-02	0.601114E+00	0.776024E+00	0.10516E+00	0.103160E+00	0.672889E-02
9	3.6	0.121316E+01	0.147468E+01	0.223013E-02	0.585204E+00	0.736897E+00	0.10019E+00	0.108800E+00	0.614413E-02
10	4.0	0.125157E+01	0.155221E+01	0.174187E-02	0.582486E+00	0.568127E+00	0.894634E-01	0.110818E+00	0.434907E-02
11	5.0	0.127966E+01	0.270432E+00	0.893751E-03	0.254634E+00	0.155946E+01	0.678681E-01	0.530293E+00	0.494329E-02
12.	6.0	0.164658E+01	0.947442E-01	0.730991E-03	0.685209E-01	0.105132E+01	0.428635E-01	0.510308E+00	0.175438E-02
13.	7.0	0.170494E+01	0.202092E+00	0.504491E-03	0.585729E+00	0.632659E+00	0.202732E-01	0.472139E+00	0.717797E-03
14.	8.0	0.186846E+01	0.299701E-01	0.460688E-03	0.197655E+00	0.430910E+00	0.119732E-01	0.489949E+00	0.176069E-02

Table S5. Computed energy levels, g tensors and tilt angles (θ) of the principal anisotropy axes of all the 8 KD's of Dy1 of **1**

Sr. No.	g_{xx}	g_{yy}	g_{zz}	Energy (cm ⁻¹)	θ (°)
1.	0.004	0.008	19.84	0	0
2.	0.06	0.1	17.44	113.29	18.47
3.	0.99	1.43	13.74	189.56	20.13
4.	5.31	5.97	8.08	262.84	18.96
5.	2.37	2.67	11.87	330.09	91.86
6.	0.29	0.42	15.38	398.8	87.08
7.	0.06	0.32	13.72	403.97	78.79
8.	0.001	0.002	19.82	571.23	57.5

Table S6. Computed energy levels, g tensors and tilt angles (θ) of the principal anisotropy axes of all the 8 KD's of Dy1A of **1**

Sr. No.	g_{xx}	g_{yy}	g_{zz}	Energy (cm ⁻¹)	θ (°)
1.	0.006	0.01	19.75	0	0
2.	0.06	0.1	17.46	109.01	19.32
3.	0.78	1.05	13.89	186.31	20.74
4.	4.82	5.7	8.58	260.71	19.35
5.	2.57	3.25	12.36	319.73	89.12
6.	0.42	1.09	14.6	382.79	89.73
7.	0.36	0.53	12.96	393.05	101.29
8.	0.003	0.004	19.73	559.76	57.37

Table S7. SINGLE ANISO computed crystal field parameters for Dy1

k	q	B_q^k
2	-2	0.003146
2	-1	-0.01373
2	0	-2.17813
2	1	4.600952
2	2	1.60213
4	-4	2.71E-05
4	-3	0.000171
4	-2	1.35E-05
4	-1	2.39E-06
4	0	-0.00278
4	1	-0.00977
4	2	0.017883
4	3	0.017089
4	4	-0.00144
6	-6	1.31E-07
6	-5	4.78E-06
6	-4	9.49E-07
6	-3	1.71E-06
6	-2	-3.2E-07
6	-1	-2.3E-07
6	0	1.31E-07
6	1	-0.00024
6	2	-5.7E-05
6	3	0.000236
6	4	0.000283
6	5	0.000317
6	6	0.000142

Table S8. SINGLE ANISO computed crystal field parameters for Dy1A

k	q	B_q^k
2	-2	-2.15E-03
2	-1	1.55E-02
2	0	-2.12E+00
2	1	4.64E+00
2	2	1.40E+00
4	-4	-2.85E-06
4	-3	-1.49E-04
4	-2	4.23E-05
4	-1	2.61E-06
4	0	-2.88E-03
4	1	-1.07E-02
4	2	1.72E-02
4	3	1.77E-02
4	4	-9.93E-04
6	-6	5.22E-08
6	-5	-5.55E-06
6	-4	3.02E-08
6	-3	-1.03E-06
6	-2	4.00E-07
6	-1	3.70E-07
6	0	1.73E-06
6	1	-2.41E-04
6	2	-6.04E-05
6	3	2.20E-04
6	4	2.84E-04
6	5	3.49E-04
6	6	1.30E-04

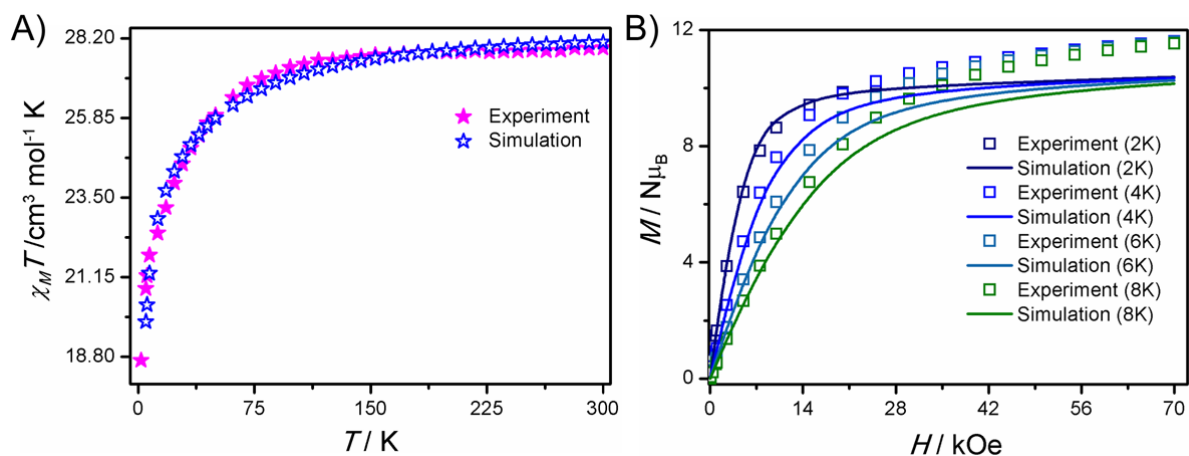


Figure S7. Poly_ANISO computed (A) magnetic susceptibility and (B) magnetization data (solid lines) with respect to experimental (scattered symbol) in complex **1**.

Table S9. Energies (cm^{-1}), g_{zz} values and tunnelling gaps (cm^{-1}) of the low-lying exchange doublet states of complex **1**

Sr. No.	g_{zz}	Δ_{tun}	Energy (cm^{-1})
1	0.99	2.08×10^{-8}	0
2	39.58	1.09×10^{-7}	0.69
3	7.55	1.48×10^{-7}	109.07
4	36.6	1.19×10^{-6}	109.64
5	7.25	2.61×10^{-7}	113.36
6	36.55	1.65×10^{-6}	113.93
7	12.13	6.15×10^{-7}	222.45
8	32.72	1.90×10^{-5}	223.85

Table S10. Magnetic entropy changes for selected Gd(III) MOF based materials:

Compound	ΔH (kOe)	$-\Delta S_m^{\max}$	References
		J Kg ⁻¹ K ⁻¹	
1. GdF ₃	20	45.5	1
	50	67.1	
	70	71.6	
2. [Gd ^{III} (OH) CO ₃] _n	30	54.4	2
	50	61.7	
	70	66.4	
3. Gd(OH) ₃	20	26.9	3
	70	62.0	
4. [Ln ₅ (μ ₃ -OH) ₅ (μ ₃ -O) (CO ₃) ₂ (HCO ₂) ₂ (C ₄ O ₄)(H ₂ O) ₂] _n	30	35.5	4
	70	60.0	
5. [Gd(HCOO) ₃] _n	20	43.7	5
	70	55.9	
6. Gd ₃ Ga ₅ O ₁₂ (GGG)	30	24.0	6
	70	38.4	
7. Complex 2	30	31.0	In this work
	50	38.4	
	70	41.6	
8. Complex 2'	30	33.7	In this work
	50	47.2	
	70	52.5	

References:

- Chen, Y.-C.; Prokleska, J.; Xu, W.-J.; Liu, J.-L.; Liu, J.; Zhang, W.-X.; Jia, J.-H.; Sechovsky, V.; Tong, M.-L., A brilliant cryogenic magnetic coolant: magnetic and magnetocaloric study of ferromagnetically coupled GdF₃. *J. Mater. Chem. C* **2015**, 3 (47), 12206.
- Chen, Y.-C.; Qin, L.; Meng, Z.-S.; Yang, D.-F.; Wu, C.; Fu, Z.; Zheng, Y.-Z.; Liu, J.-L.; Tarasenko, R.; Orendac, M.; Prokleska, J.; Sechovsky, V.; Tong, M.-L., Study of a magnetic-cooling material Gd(OH)CO₃. *J. Mater. Chem. A* **2014**, 2 (25), 9851.
- Yang, Y.; Zhang, Q.-C.; Pan, Y.-Y.; Long, L.-S.; Zheng, L.-S., Magnetocaloric effect and thermal conductivity of Gd(OH)₃ and Gd₂O(OH)₄(H₂O)₂. *Chem. Commun.* **2015**, 51 (34), 7317.
- Biswas, S.; Mondal, A. K.; Konar, S., Densely Packed Lanthanide Cubane Based 3D Metal-Organic Frameworks for Efficient Magnetic Refrigeration and Slow Magnetic Relaxation. *Inorg. Chem.* **2016**, 55 (5), 2085.
- Lorusso, G.; Sharples, J. W.; Palacios, E.; Roubeau, O.; Brechin, E. K.; Sessoli, R.; Rossin, A.; Tuna, F.; McInnes, E. J. L.; Collison, D.; Evangelisti, M., A dense metal-organic framework for enhanced magnetic refrigeration. *Adv. Mater.* **2013**, 25 (33), 4653.
- Daudin, B.; Lagnier, R.; Salce, B., Thermodynamic properties of the gadolinium gallium garnet, Gd₃Ga₅O₁₂, between 0.05 and 25 K. *J. Magn. Magn. Mater.* **1982**, 27 (3), 315.